Cellular/Molecular

Channel-Mediated Lactate Release by K^+-Stimulated Astrocytes

Tamara Sotelo-Hitschfeld,[1,4] María I. Niemeyer,[1] Philipp Mächler,[2,3] Iván Ruminot,[1] Rodrigo Lerchundi,[1,4] Matthias T. Wyss,[2,3] Jillian Stobart,[2,3] Ignacio Fernández-Moncada,[1,4] Rocío Valdebenito,[1] Pamela Garrido-Gerter,[1,4] Yasna Contreras-Baeza,[1,4] Bernard L. Schneider,[5] Patrick Aebischer,[5] Sylvain Lengacher,[5] Alejandro San Martín,[1,4] Juliette Le Douce,[6] Gilles Bonvento,[6] Pierre J. Magistretti,[5,7] Francisco V. Sepúlveda,[1] Bruno Weber,[2,3] and L. Felipe Barros[1]

[1]Centro de Estudios Científicos, Valdivia 5110466, Chile, [2]Institute of Pharmacology and Toxicology, University of Zürich, 8057 Zürich, Switzerland, [3]Neuroscience Center Zürich, University and ETH Zürich, 8092 Zürich, Switzerland, [4]Universidad Austral de Chile, Valdivia, Chile, [5]Brain Mind Institute, École Polytechnique Fédérale de Lausanne, CH-1015 Lausanne, Switzerland, [6]Commissariat à l'Energie Atomique, Institut d'Imagerie Biomédicale, Molecular Imaging Research Center and Centre National de la Recherche Scientifique, Université Paris-Sud, Université Paris-Saclay, UMR 9199, F-92265 Fontenay-aux-Roses, France, and [7]Division of Biological and Environmental Sciences and Engineering, Kaust, Saudi Arabia

Excitatory synaptic transmission is accompanied by a local surge in interstitial lactate that occurs despite adequate oxygen availability, a puzzling phenomenon termed aerobic glycolysis. In addition to its role as an energy substrate, recent studies have shown that lactate modulates neuronal excitability acting through various targets, including NMDA receptors and G-protein-coupled receptors specific for lactate, but little is known about the cellular and molecular mechanisms responsible for the increase in interstitial lactate. Using a panel of genetically encoded fluorescence nanosensors for energy metabolites, we show here that mouse astrocytes in culture, in cortical slices, and *in vivo* maintain a steady-state reservoir of lactate. The reservoir was released to the extracellular space immediately after exposure of astrocytes to a physiological rise in extracellular K^+ or cell depolarization. Cell-attached patch-clamp analysis of cultured astrocytes revealed a 37 pS lactate-permeable ion channel activated by cell depolarization. The channel was modulated by lactate itself, resulting in a positive feedback loop for lactate release. A rapid fall in intracellular lactate levels was also observed in cortical astrocytes of anesthetized mice in response to local field stimulation. The existence of an astrocytic lactate reservoir and its quick mobilization via an ion channel in response to a neuronal cue provides fresh support to lactate roles in neuronal fueling and in gliotransmission.

Key words: **fluorescence microscopy; genetically encoded nanosensor; gliotransmission; membrane depolarization**

Introduction

The discovery of surface lactate receptors in neurons and other brain cells (Bozzo et al., 2013; Lauritzen et al., 2013; Tang et al., 2014) has rekindled interest in the local extracellular lactate rise that develops within seconds of neural activation (Prichard et al., 1991; Hu and Wilson, 1997; Barros, 2013). Some of us have recently proposed a mechanism contributing to the lactate transient that is based on the observation that a rise in extracellular K^+ ($[K^+]_o$), such as that recorded during neural activity, stimulates an astrocytic glucose consumption in culture and in brain slices, which also occurs within seconds (Bittner et al., 2011; Ruminot et al., 2011). Exposure of astrocytes to elevated $[K^+]_o$ was found to augment extracellular lactate, but, given the limited temporal resolution of standard biochemical techniques, it was not possible to ascertain whether K^+-stimulated astrocytes were able to release lactate within seconds, the time frame of the interstitial lactate transient observed *in vivo*. Genetically encoded nanosensors specific for nicotinamide adenine dinucleotide (NADH), lactate, and pyruvate, which were used here to map the fate of glucose and lactate during the first seconds of K^+ stimulation, have been developed since then (Hung et al., 2011; San Martín et al., 2013, 2014a). We report that astrocytes *in vitro* and *in vivo* maintain a cytosolic reservoir of lactate, which, in response to plasma membrane depolarization, is immediately released to the extracellular space via an ion channel that conducts lactate and is positively modulated by lactate itself.

Received Dec. 11, 2014; revised Jan. 9, 2015; accepted Jan. 13, 2015.

Author contributions: T.S.-H., M.I.N., M.T.W., F.V.S., B.W., and L.F.B. designed research; T.S.-H., M.I.N., P.M., I.R., R.L., M.T.W., I.F.-M., R.V., P.G.-G., Y.C.-B., A.S.M., and J.L.D. performed research; J.S., B.L.S., P.A., S.L., A.S.M., J.L.D., G.B., P.J.M., B.W., and L.F.B. contributed unpublished reagents/analytic tools; T.S.-H., M.I.N., P.M., I.R., R.L., M.T.W., I.F.-M., R.V., P.G.-G., Y.C.-B., A.S.M., F.V.S., B.W., and L.F.B. analyzed data; T.S.-H., F.V.S., B.W., and L.F.B. wrote the paper.

This research was partly funded by Fondecyt Grant 1130095 (to L.F.B.) and a joint grant from the Comisión Nacional de Investigación Científica y Tecnológica (CONICYT)-Chile and the Deutsche Forschungsgemeinschaft to L.F.B. and Joachim W. Deitmer, TU Kaiserslautern, Germany (DFG-12, DE 231/25-1). B.W. is partly supported by the Clinical Research Priority Program of the University of Zurich on Molecular Imaging. We also thank the Evaluation-orientation de la Coopération Scientifique-Sud program (Grant C10S04 to G.B. and L.F.B.) and the French National Research Agency ANR (Grant 2011 MALZ 003-02 to G.B.). The Centro de Estudios Científicos is funded by the Chilean Government through the Centers of Excellence Basal Financing Program of CONICYT. We thank Pablo Cid for helpful discussions, Karin Alegría for expert technical assistance, and Karen Everett for critical reading of the manuscript.

The authors declare no competing financial interests.

Correspondence should be addressed to L. Felipe Barros, Centro de Estudios Científicos (CECs), Valdivia 5110466, Chile. E-mail: fbarros@cecs.cl.

DOI:10.1523/JNEUROSCI.5036-14.2015

 0270-6474/15/354168-11$15.00/0

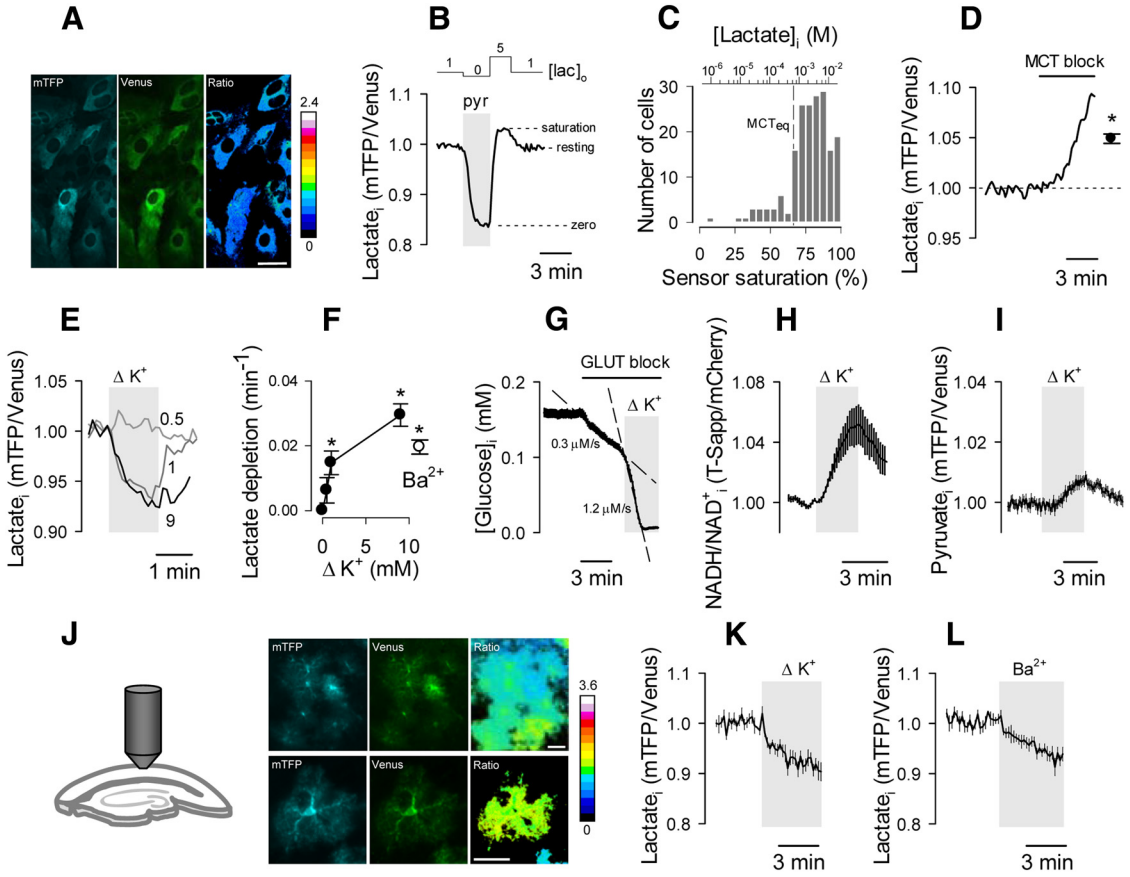

Figure 1. Astrocytes maintain a cytosolic lactate reservoir that is depleted in the short term by high $[K^+]_o$. ***A***, The FRET lactate sensor Laconic expressed in the cytosol of cultured astrocytes, showing mTFP (blue), Venus (green), and the ratio between mTFP and Venus. Scale bar, 20 μm. ***B***, Laconic was first depleted of lactate by superfusion with 10 mM pyruvate (pyr), and then saturated with 5 mM lactate and 2 mM glucose (San Martín et al., 2013). ***C***, Resting lactate level in 183 cells (17 experiments), estimated with the protocol in ***B***. The top *x*-axis indicates lactate concentration, according to the kinetic parameters estimated *in vitro*. Equilibrium concentration (MCT_{eq}) of the monocarboxylate transporters. ***D***, Response of intracellular lactate to 1 μM AR-C155858. The closed symbol represents the average change after 5 min of MCT blockage. ***E***, Effect of 0.5, 1, and 9 mM $[K^+]_o$ additions on the lactate level of an astrocyte. Resting $[K^+]_o = 3$ mM. ***F***, Initial rates of K^+-induced lactate depletion. The open symbol represents the initial rate of lactate depletion after exposure to 3 mM Ba^{2+}. ***G–I***, Effect of a 9 mM $[K^+]_o$ rise on glucose consumption (***G***), cytosolic $NADH/NAD^+$ ratio (***H***), and cytosolic pyruvate level (***I***). ***J***, Protoplasmic astrocytes expressing Laconic observed in an acute cortical slice at low (top) and high (bottom) magnification. Scale bar, 20 μm. ***K***, ***L***, The effects of increasing $[K^+]_o$ by 9 mM (***K***) or by adding 3 mM Ba^{2+} (***L***) on the lactate level of protoplasmic astrocytes are shown.

Materials and Methods

Standard reagents and inhibitors were acquired from Sigma. AR-C155858 was purchased from Haoyuan Chemexpress. Plasmids encoding the sensors FLII ^{12}Pglu700$\mu\Delta$6 (Takanaga et al., 2008), Peredox (Hung et al., 2011), Laconic (San Martín et al., 2013), and Pyronic (San Martín et al., 2014a) are available from Addgene (www.addgene.org). Ad Laconic, Ad Pyronic, and Ad FLII ^{12}Pglu700$\mu\Delta$6 (all serotype 5) were custom made by Vector Biolabs. The adeno-associated virus (AAV9) expressing Laconic under the control of the short gfaABC$_1$D promoter was generated at the École Polytechnique Fédérale de Lausanne. Design, production, and titration of the AAV9 vector for transgene expression in astrocytes have been described previously (Dirren et al., 2014).

Animals

Animal procedures in Valdivia were approved by the Centro de Estudios Científicos Animal Care and Use Committee, following the recommendations of the *Guide for the Care and Use of Laboratory Animals*, Institute of Laboratory Animal Resources, National Research Council. Animals used were mixed F1 male mice (C57BL/6J6CBA/J), kept in an animal room under specific pathogen-free conditions at a room temperature of 20 ± 2°C, in a 12 h light/dark cycle with free access to food and water. Surgical and experimental procedures in Zürich were approved by the local veterinary authorities, conforming to the guidelines of the Swiss Animal Protection Law, Veterinary Office, Canton Zürich (Act of Animal Protection 16 December 2005 and Animal Protection Ordinance 23 April 2008). Wild-type mice (C57BL/6J; Harlan Laboratories) 10 weeks of age and with a body weight of 20 g were housed in single cages, with water and food available *ad libitum*.

Experimental preparations

Culture cells. Mixed cortical cultures of neuronal and glial cells were prepared from 1- to 3-d-old neonates (Loaiza et al., 2003). HEK293 cells were cultured as previously described (San Martín et al., 2013). HEK cells and astrocytes were plasmid transfected (0.5 μg/ml) using Lipofectamine 2000 or 3000 (Life Technologies). Alternatively, astrocytes were exposed to 5×10^6 pfu of Ad Laconic, Ad Pyronic, or Ad FLII ^{12}Pglu700$\mu\Delta$6, and were studied after 48 h (culture days 8–10). Extracellular lactate levels were measured with the BioVision Lactate Assay Kit according to the instructions of the manufacturer.

Brain slices. Neonatal mice (days 1–3) were removed from the mother and anesthetized by hypothermia over 15 min. Animals were positioned upon a stage and injected with 1 μl of AAV9 (titer 3.1E12 VG/ml) into the skull (Davidson et al., 2010) using a Fusion 100 syringe pump (Chemyx). After injection, the animals were positioned on a temperate bed until they recovered and then returned to the mother. After 4 weeks, animals were killed by cervical dislocation and coronal brain sections (200 μm in thickness) were prepared as described previously (Jakoby et al., 2014).

Somatosensory cortex in vivo. Animals were anesthetized with an intraperitoneally injected mixture of fentanyl (0.05 mg/kg body weight; Sintenyl, Sintetica), midazolam (5 mg/kg body weight; Dormicum, Roche), and medetomidine (0.5 mg/kg body weight; Domitor, Orion Pharma), and again after 50 min with midazolam only (5 mg/kg body weight). If

necessary, anesthesia was prolonged with isoflurane (0.5%; Abbott). The animal head was fixed in a stereotaxic apparatus (David Kopf Instruments), and the eyes were kept wet with an ointment (vitamin A eye cream; Bausch & Lomb). A 4 × 4 mm craniotomy was performed using a surgical drill (Osseodoc) and 200 nl of recombinant AAV9 (titer 3.1E12 VG/ml), carrying the genetically encoded lactate sensor Laconic, was injected into the primary somatosensory cortex. A square coverslip (3 × 3 mm, UQG Optics Ltd) was lightly pressed onto the exposed brain and fixed with dental cement to the skull. A bonding agent (Gluma Comfort Bond, Heraeus Kulzer) was applied to the cleaned skull and was polymerized with a handheld blue light source (600 mW/cm^2; Demetron LC). A custom-made aluminum headpost was fixed to the bonding agent with dental cement (Tetric EvoFlow, Ivoclar Vivadent). The open skin was treated with an antibiotic ointment (Cicatrex, Janssen-Cilag) and closed with acrylic glue (Histoacryl, B. Braun). After surgery the animals were kept warm and given analgesics (Novaminsulfon, 50%, Sintetica), and the antibiotic enrofloxacin was added to the drinking water for 5 d (200 mg/L drinking water; Baytril, Bayer).

Fluorescence imaging

Detailed protocols for the use of the fluorescent sensors are available (Hou et al., 2011; Tantama et al., 2012; Barros et al., 2014; San Martín et al., 2014b). In the article describing the lactate sensor Laconic (San Martín et al., 2013), data were presented showing some sensitivity to pH in the alkaline range and also to citrate in the millimolar range. However, further characterization has shown that the sensitivities to pH and citrate were not a property of the sensor itself but *in vitro* artifacts respectively due to protein instability at room temperature in a noncellular milieu and divalent chelation by citrate. These results will be presented in detail in a separate manuscript (San Martin et al., manuscript in preparation). Measurements in cultured cells were performed at room temperature (22–24°C) in a 95% air/5% CO_2-gassed solution of the following composition (in mM): 112 NaCl, 3 KCl, 1.25 CaCl2, 1.25 MgCl2, 1–2 glucose, 10 HEPES, and 24 NaHCO3, pH 7.4. Slice measurements were performed at room temperature (22–24°C) in a 95% O_2/5% CO_2-gassed solution of the following composition (in mM): 126 NaCl, 3 KCl, 1.25 NaH_2PO_4, 1.25 CaCl2, 1.25 MgCl2, 10 glucose, and 26 NaHCO3, at pH 7.4. Cells and slices were imaged with an upright Olympus FV1000 confocal microscope equipped with a 20× water-immersion objective (numerical aperture, 1.0) and a 440 nm solid-state laser. Alternatively, cells were imaged with Olympus IX70 or BX51 microscopes equipped with Cairn Research monochromators and Optosplits, and either a Hamamatsu Orca or Rollera camera. FLII ^{12}Pglu700$\mu\Delta$6, Laconic, and Pyronic were excited at 430 nm for 0.2–0.8 s, and were detected at 485/40 nm [cyan fluorescent protein or monomeric teal fluorescent protein (mTFP)] and 535/30 nm (Citrine or Venus). Peredox-mCherry was imaged at 410 nm excitation and 485/40 emission (T-sapphire), and 570 nm excitation and 610/50 nm emission (mCherry). Masked ratio images were generated from background-subtracted images using ImageJ software. The H^+-sensitive dye 2′,7′-bis-(2-carboxyethyl)-5-(and-6)-carboxyfluorescein (BCECF) was ester loaded at 0.1 μM for 3–4 min, and the signal was calibrated by exposing the cultures to solutions of different pH after permeabilizing the cells with 10 μg/ml nigericin and 20 μg/ml gramicidin in an intracellular buffer. BCECF was sequentially excited at 440 and 490 nm (0.05 s), and imaged at 535/30 nm. Calcein was ester loaded at 0.1 μM for 20 min and then imaged using confocal microscopy.

After 3 weeks of sensor expression, living mice were imaged with a custom-built two-photon laser-scanning microscope using a tunable pulsed (Mai Tai eHP DS system, Spectra-Physics) at a wavelength of 870 nm using a 20× water-immersion objective (W Plan-Apochromat 20×/1.0 differential interference contrast, Zeiss). The animals were head fixed and kept under anesthesia, as described above. Body temperature was kept constant with a feedback-controlled heating pad (37°C; Harvard Apparatus). Frame scans were acquired with ScanImage (r3.8.1; Janelia Research Campus; Pologruto et al., 2003) at 1.63 Hz and 512 × 512 pixels resolution. Single astrocytes of cortical layers L2/3 (150–250 μm below the dura) were outlined using ImageJ (1.46r; National Institutes of Health) and the mTFP channel (with bandpass filter 475/64; Semrock)

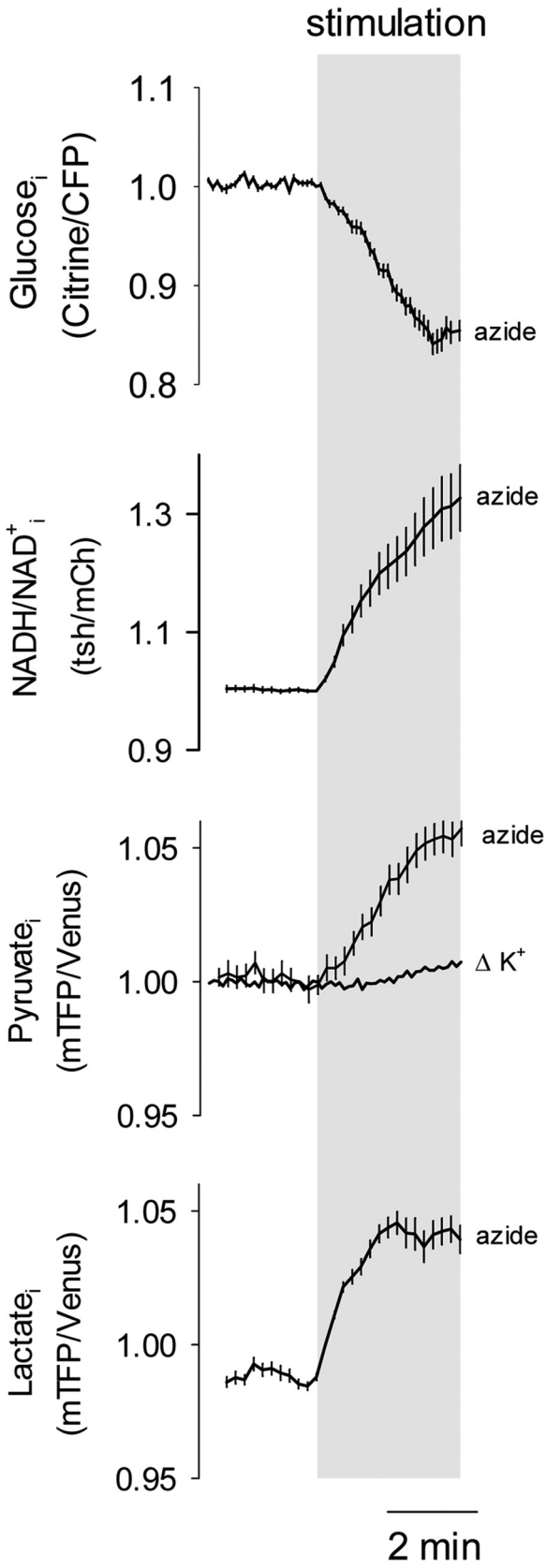

Figure 2. Intracellular lactate accumulation in response to OXPHOS inhibition. Astrocytes were exposed to 5 mM azide while measuring glucose, NADH/NAD $^+$ ratio, pyruvate or lactate. The effect of 12 mM $[K^+]_o$ on pyruvate levels (from Fig. 1*I*) is shown for comparison.

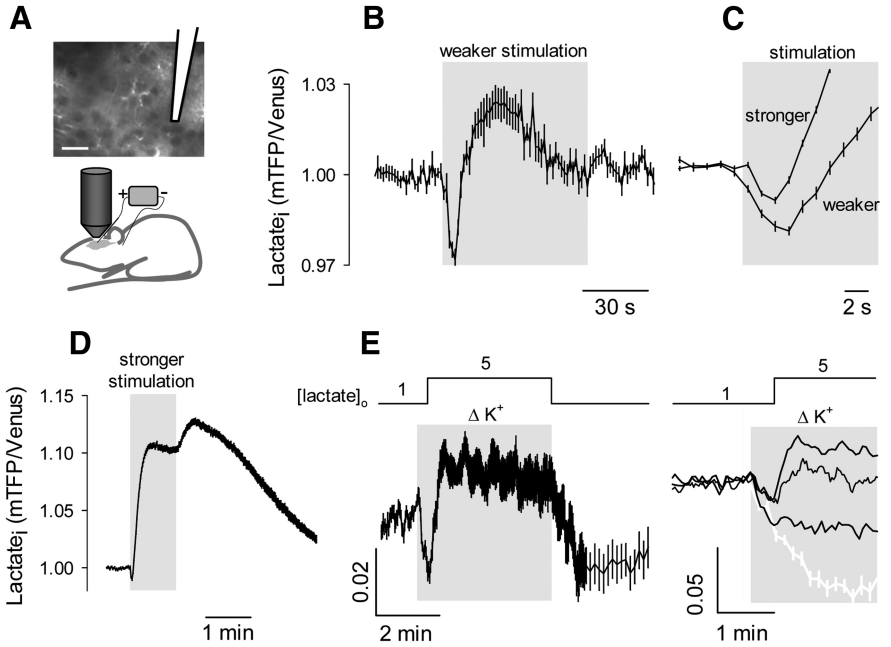

Figure 3. Early depletion of astrocytic lactate during local electrical stimulation *in vivo*. The strength of electrical stimulation was modulated by varying the distance between cells and the tip of the stimulation pipette, giving a weaker stimulation at 300–500 μm and a stronger stimulation at 20–200 μm. ***A***, Imaging of Laconic expressed in somatosensory cortex astrocytes. The location of the stimulation pipette is indicated. Scale bar, 20 μm. ***B***, Data from a single experiment. ***C***, Early response to weaker ($n = 3$ experiments) and stronger stimulation ($n = 7$ experiments). ***D***, Extended time course for stronger stimulation ($n = 7$ experiments) ***E***, Left, Intracellular lactate level in cultured astrocytes exposed first to a 9 mM increase in $[K^+]_o$, and 30 s later, to a rise in extracellular lactate level from 1 to 5 mM. Right, Data from three cells from the same field (black) are compared with the average depletion elicited by a 9 mM $[K^+]_o$ increase at constant extracellular lactate concentration of 1 mM (white).

was divided by the Venus channel (with bandpass filter 542/50; Semrock), and the ratio was normalized to the corresponding baseline using Matlab (MathWorks). Glass capillaries (Science Products; GB120F-8P 0.69 × 1.20 × 80 mm with filament) were pulled to achieve an impedance of 1.5 MΩ at 1 kHz (P-87 pipette puller, Sutter Instrument Co.) and were filled with an artificial CSF solution of the following composition (in mM): 125 NaCl, 2.5 KCl, 2 CaCl2, 1 MgCl2, 25 glucose, 1.25 NaH_2PO_4, and 25 NaHCO3, pH 7.4 (Laboratorium Dr. Bichsel AG, Interlaken, Switzerland). The glass of the cranial window was split using a diamond glass cutter and was partially removed. The pipette was mounted on a manipulator (SM-5, Luigs & Neumann) inserted under visual control and left to rest for 60 min before imaging. Intracortical microstimulation was applied with a DC cathodal current of 100 μA for 1 min (1 Hz train frequency, 100 ms trains at 330 Hz, 0.26 ms pulse width) using a constant-current isolator (STG 4002, Multi Channel Systems).

Electrophysiology

Culture dishes containing cortical astrocytes were transferred to the stage of an inverted microscope for study. They were continuously superfused with a bathing solution containing the following (in mM): 136 NaCl, 3 KCl, 1.25 MgCl2, 1.25 CaCl2, 2.0 Glucose, 1.0 NaLactate, and 10 HEPES-Tris, at pH 7.4 and osmolality of 300 mOsm. The pipette solution contained the following (in mM): 145 NaLactate, 1.0 NaCl, 3.0 KCl, 3.0 BaCl2, and 10 HEPES-Tris 10 mM, at pH 7.4 and osmolality of 300 mOsm. Recordings of single channels in the cell-attached patch-clamp configuration were performed using 6- to 12-d-old astrocytes. Patch pipettes made from borosilicate glass were fire polished and covered in beeswax, and had a tip resistance of 3–4 MΩ (measured using the pipette solution described above). After obtaining GΩ seals, currents were measured using a List Medical L/M-EPC5 amplifier. An Ag/AgCl pellet acted as a bath ground and was connected to the bathing solution via a 0.5 M KCl agar bridge. Potentials were corrected for liquid junction shifts (Barry, 1994). Acquisition and analysis were performed with a Digidata 1200A analog-to-digital converter and Clampfit version 9.0 software (Molecular Devices). Acquisition was at 10 kHz with a filter (four-pole Bessel filter) at 3 kHz. Experiments were conducted at room temperature (20–24°C). NP_o, where N is the number of active channels in the membrane patch and P_o is the open probability, was calculated using the single-channel search and event statistics algorithms in pClamp version 9.0 software. The mean current I passing through the N channels present in the patch was estimated from current amplitude histograms. Single-channel conductance estimates were made on the assumption that astrocytes had a membrane potential E_m of −80 mV (Ruminot et al., 2011). Intracellular lactate concentration was assumed to be 1.4 mM. An intracellular chloride concentration of 30 mM was assumed (Bekar and Walz, 2002). We used these concentrations to calculate cell-attached patch reversal potential E_{rev} values of 27 and −116 mV, respectively, for chloride and lactate.

Data presentation and statistical analysis

Line traces represent individual cells. Unless otherwise stated, traces with error bars correspond to the mean ± SEM of eight or more cells ($n \geq 3$ experiments). Differences in mean values of paired samples were evaluated with the Student's t test. p values of <0.05 were considered significant and are indicated with an asterisk (*).

Results

Resting astrocytes maintain a standing lactate reservoir

Astrocyte lactate dynamics were monitored in real time with Laconic, the Forster resonance energy transfer (FRET) lactate nanosensor (San Martín et al., 2013; Fig. 1*A*). To estimate resting lactate levels in cultured astrocytes, cells were first emptied of lactate by accelerated exchange with pyruvate and then exposed to saturating levels of lactate, a two-point calibration protocol that has been described in detail previously (San Martín et al., 2013). With this approach, the sensor was found to be close to saturation in most astrocytes (Fig. 1*B*,*C*). Using the kinetic parameters obtained *in vitro* (San Martín et al., 2013), the average concentration of cytosolic lactate was estimated to be 1.4 ± 0.02 mM ($n = 183$ cells in 17 experiments). The transport of lactate across the astrocytic plasma membrane is mediated by monocarboxylate transporters (MCTs) that catalyze the electroneutral cotransport of a lactate anion and an H^+ ion. With 1 mM lactate in the superfusate at a pH of 7.4, and a mean intracellular pH of 7.2 ± 0.02 ($n = 43$ cells 3 experiments), MCTs in astrocytes are at thermodynamic equilibrium at 0.63 mM intracellular lactate ($[lactate]_o \times [H^+]_o = [lactate]_i \times [H^+]_i$). As shown in Figure 1*C*, 88% of the astrocytes maintained cytosolic lactate levels above equilibrium in the resting condition. MCT blockage with AR-C155858 (Ovens et al., 2010) led to further intracellular lactate accumulation (Fig. 1*D*), providing independent evidence that resting astrocytes are tonic lactate producers that keep lactate above the MCT equilibrium.

Depolarization by high $[K^+]_o$ depletes astrocytic lactate

A rise in $[K^+]_o$ has been reported to stimulate astrocytic glucose consumption, glycogen mobilization, and lactate production in cell cultures and in tissue slices (Hof et al., 1988; Bittner et al.,

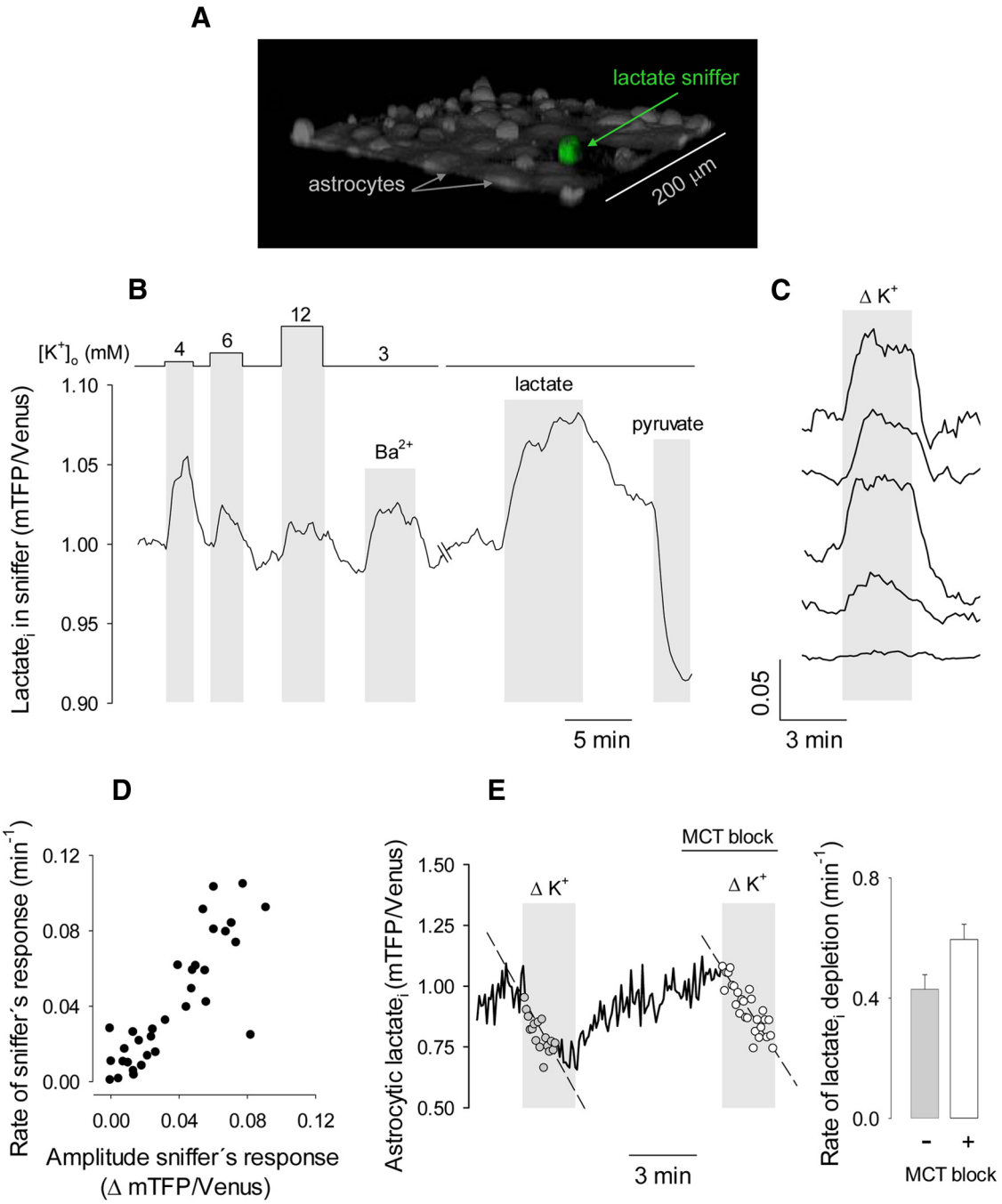

Figure 4. Fast astrocytic lactate release detected with a lactate sniffer. ***A***, HEK293 cells expressing Laconic (sniffers) were seeded on top of an astrocytic culture and imaged by 3D confocal microscopy (green). A second 3D reconstruction was performed after ester loading the culture with calcein (gray). ***B***, Response of a sniffer positioned on top of an astrocytic culture to increasing concentrations of $[K^+]_o$ (4, 6, and 12 mM), 3 mM Ba^{2+}, 1 mM lactate, and 10 mM pyruvate. The experiment was performed in 2 mM glucose and 0 mM lactate. ***C***, Typical response of sniffers to astrocytic culture exposure to 12 mM K^+. ***D***, Correlation between the amplitude and the initial rate of the response of the sniffer to 12 mM K^+. ***E***, Astrocytic lactate depletion by 12 mM K^+ in the absence (gray symbols and bars) and presence (white symbols and bars) of 1 μM AR-C155858.

2011; Ruminot et al., 2011; Choi et al., 2012; Sotelo-Hitschfeld et al., 2012). Therefore, we expected to find increased cytosolic lactate levels in K^+-stimulated astrocytes. Paradoxically, high $[K^+]_o$ led to depletion of the cytosolic lactate reservoir (Fig. 1*E*). The phenomenon was evoked with 4 mM K^+, a mere 1 mM over resting $[K^+]_o$ (Fig. 1*E*,*F*) and within the range reported in brain interstice during physiological neural activity (Fröhlich et al., 2008). The effect of K^+ was mimicked by Ba^{2+} (Fig. 1*F*), which depolarizes the plasma membrane by blocking K^+ channels (Ruminot et al., 2011). As reported (Bittner et al., 2011), the measurement of glucose consumption by applying a glucose transporter GLUT blocker (Bittner et al., 2010) to astrocytes expressing the glucose nanosensor FLII^{12}Pglu700$\mu\Delta$6 (Takanaga et al., 2008) showed that high $[K^+]_o$ stimulated glycolysis by >300% (Fig. 1*G*). Consistent with an increased glycolytic rate, Peredox (Hung et al., 2011) showed an increased NADH/NAD^+ ratio (Fig. 1*H*). However, Pyronic (San Martín et al., 2014a) revealed that cytosolic pyruvate concentrations increased slightly and only after a delay of ~30 s (Fig. 1*I*). The weak response of pyruvate to such strong glycolytic activation is consistent with the

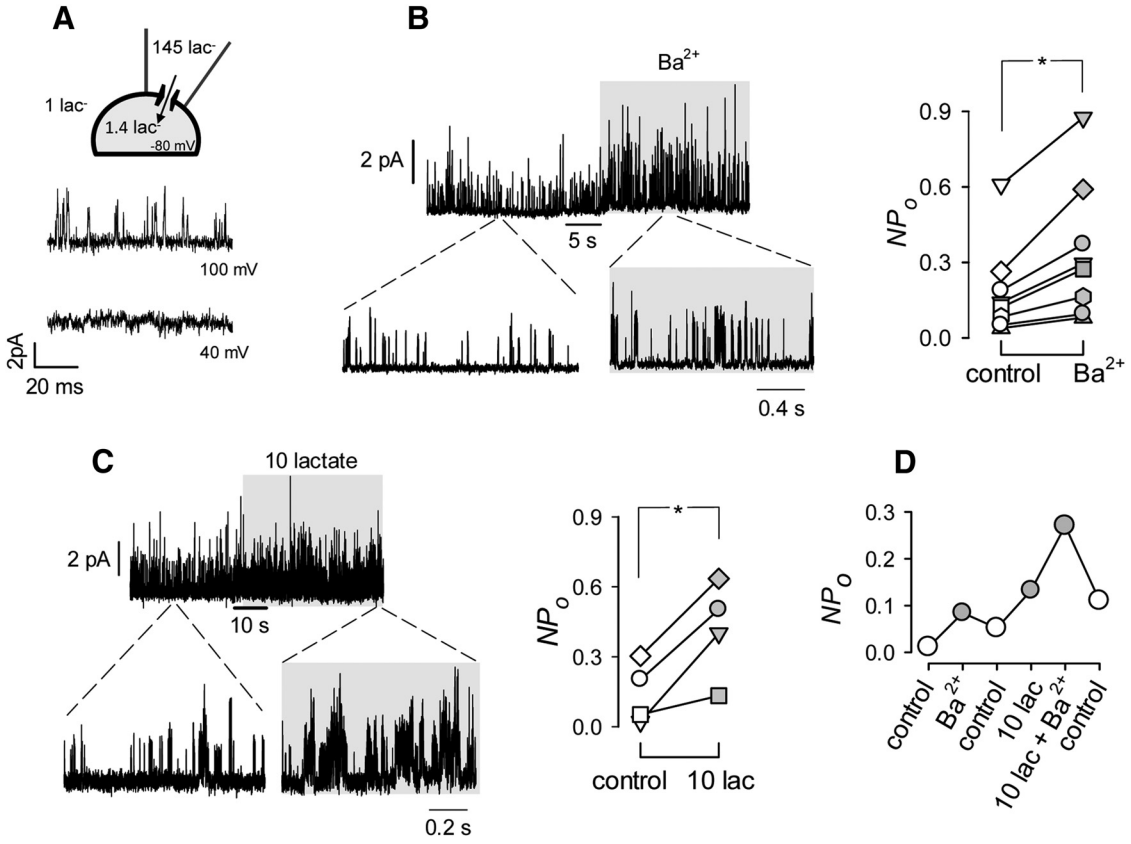

Figure 5. A lactate-permeable channel modulated by membrane depolarization and lactate. ***A***, Traces obtained under lactate-rich (145 mM) and chloride-low (10 mM) pipette conditions in the cell-attached mode at 100 and 40 mV applied potential. ***B***, Left, Recording from an astrocyte patch held at 0 mV (80 mV applied potential) before and during exposure of the cell to 3 mM Ba^{2+}. Right, The channel activity in eight similar experiments is illustrated as NP_o, the product of the number of channels in the patch and the open probability of each channel. ***C***, Left, Effect of increasing bath lactate concentration from 1 to 10 mM on channel activity. Right, Summary of four similar experiments. ***D***, A cell was sequentially bathed with 3 mM Ba^{2+} and/or 10 mM lactate for periods of 5 min as shown.

simultaneous operation of a lactate dehydrogenase (LDH)-mediated pyruvate sink driven by the lactate depletion and NADH increase. The phenomenon of lactate depletion seemed specific to high $[K^+]_o$, as the inhibition of oxidative phosphorylation (OXPHOS), which also stimulated glycolysis and increased the cytosolic NADH/NAD^+ ratio, led to the expected immediate accumulation of both pyruvate and lactate (Fig. 2). To study astrocytes in the tissue context, a recombinant adeno-associated virus coding for Laconic under the short $gfaABC_1D$ promoter was stereotaxically injected into the brain of neonatal mice, followed by cortical slice preparation and FRET determinations 4 weeks later. As illustrated in Figure 1*J–L*, when the slice was exposed to high $[K^+]_o$ or Ba^{2+}, protoplasmic astrocytes responded with a lactate depletion similar to that observed in culture. Considering the responses in cultured cells and in tissue slices of lactate, glucose, NADH/NAD^+ ratio, and pyruvate, we hypothesized that astrocytic depolarization by high $[K^+]_o$ stimulated lactate release to a larger extent than glycoytic lactate production.

Lactate dynamics *in vivo*

The lactate sensor was expressed in astrocytes of the primary somatosensory cortex of adult mice using the adeno-associated viral vector and was then imaged under anesthesia through a cranial window with two-photon microscopy (Fig. 3*A*). Local field stimulation that increases $[K^+]_o$ *in vivo* and depolarizes astrocytes within seconds (Chesler, 2003; Fröhlich et al., 2008) elicited a complex astrocytic lactate response. Immediately after the onset of stimulation, there was a fast transient decrease, followed by an overshoot and a secondary decrease despite continued stimulation (Fig. 3*B*). The lactate dip does not seem to arise from a stimulation artifact, as astrocytes located near the stimulation pipette showed a smaller dip (Fig. 3*C*). This stronger stimulation provoked a faster and larger overshoot that maintained cytosolic lactate above baseline levels long after stimulation had ended (Fig. 3*D*). Whereas electrical stimulation may affect metabolism by several mechanisms, a possible interpretation for the complex response observed *in vivo* is that the initial lactate dip is mediated by high $[K^+]_o$, as observed *in vitro*, and that the overshoot reflects the interstitial lactate buildup known to occur *in vivo*. Consistent with this explanation, both dip and overshoot could be mimicked in cultured astrocytes by elevating extracellular lactate levels a few seconds after the application of K^+ (Fig. 3*E*). The effect of adding lactate was variable from cell to cell, ranging from a slight decrease in the rate of lactate depletion to a proper overshoot (Fig. 3*E*). In view of the results described below, this is likely explained by variable balancing between MCT-mediated lactate influx and channel-mediated lactate efflux.

Astrocytes release lactate within seconds of membrane depolarization

Augmented lactate efflux in response to astrocyte depolarization was first confirmed with an enzymatic assay, which showed that a 1 min exposure of cultured astrocytes to 12 mM $[K^+]_o$ increased extracellular lactate by 69 ± 7%. For better temporal resolution,

a lactate-sniffer cell was engineered by expressing Laconic in wild-type HEK293 cells, which are MCT rich (San Martín et al., 2013, 2014a) and insensitive to glycolytic modulation by K^+ (Ruminot et al., 2011). To estimate lactate levels in the immediate vicinity of astrocytes, lactate sniffer cells were seeded on top of the astrocytic monolayer (Fig. 4*A*). Within seconds of exposing the cultures to elevated $[K^+]_o$ or Ba^{2+} level, the sniffers detected a higher extracellular lactate (Fig. 4*B*). The typical response was a rapid rise to a new steady state, which reverted to baseline levels after agonist removal, although we saw considerable cell-to-cell variability (Fig. 4*C*,*D*). Control experiments in the absence of astrocytes showed that intracellular lactate in HEK293 cells was insensitive to 12 mM $[K^+]_o$ or 3 mM Ba^{2+} (data not shown). These results indicate that astrocytes release lactate within seconds of membrane depolarization, thus explaining the intracellular depletion despite glycolytic stimulation. Next, we focused on the mechanisms underlying the lactate release, with first possible candidates being MCTs. However, the MCT blocker AR-C155858, which abrogates lactate permeation in these cells (San Martín et al., 2013, 2014a), had no apparent effect on the lactate depletion (Fig. 4*E*), pointing to the existence of an alternative release pathway.

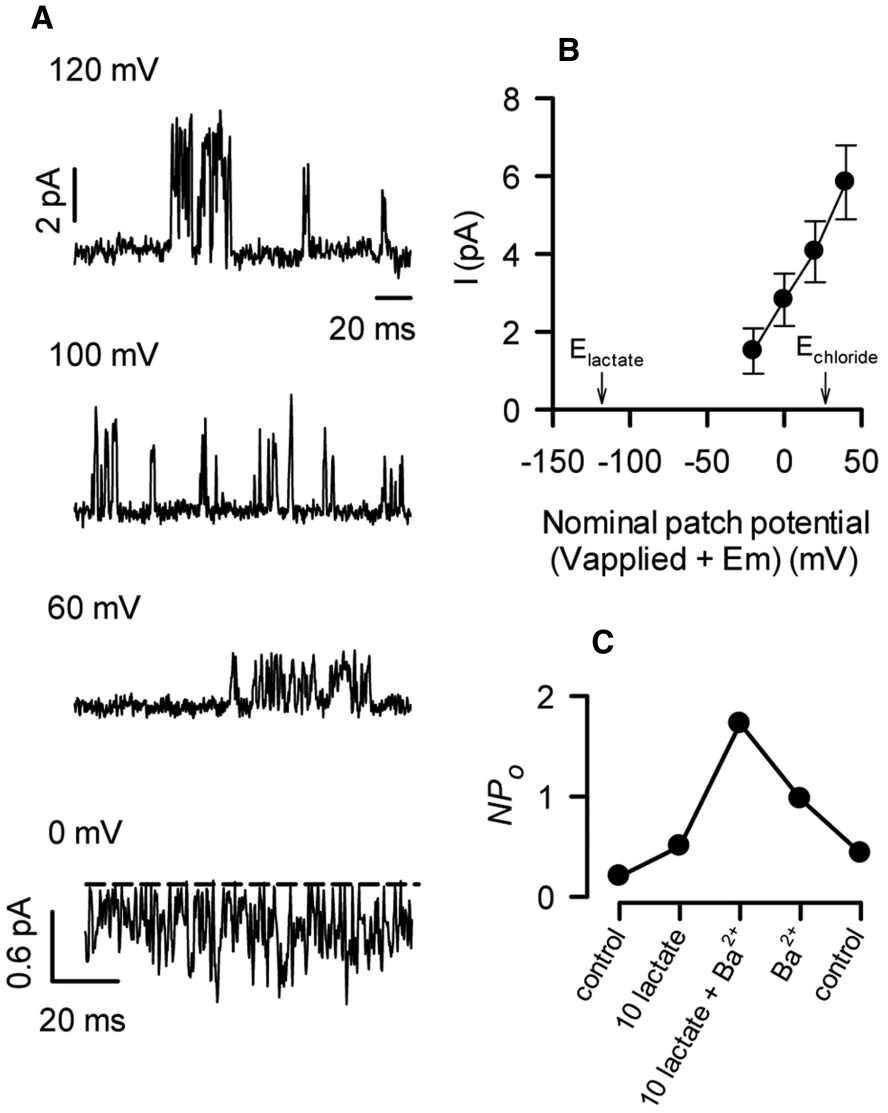

Figure 6. Further characterization of the lactate-permeable channel. ***A***, Traces obtained with a lactate-rich (145 mM), chloride-low (10 mM) medium, with pipette in the cell-attached mode at 120, 100, 60, and 0 applied potential. ***B***, Single-channel current obtained at increasing nominal patch potentials (calculated assuming an astrocytic membrane potential of −80 mV). The equilibrium potentials estimated for lactate and chloride are indicated. ***C***, A cell was sequentially bathed with 10 mM lactate and 3 mM Ba^{2+} for periods of 5 min as shown.

Channel-mediated lactate release by astrocytes

Our search for a lactate conductance started with whole-cell patch-clamp experiments, but no significant currents could be detected with a lactate-rich pipette at resting membrane potential or during depolarization ($n = 6$ experiments, data not shown). Experiments were therefore performed in the cell-attached configuration, a minimally invasive approach that leaves the intracellular milieu unperturbed, using a pipette solution rich in lactate, low in chloride, and supplemented with 3 mM Ba^{2+} to eliminate the potassium conductance (Ruminot et al., 2011). Assuming intracellular concentrations of 1.4 mM for lactate (see above) and of 30 mM for chloride (Bekar and Walz, 2002), approximate lactate reversal potential $E_{lactate}$ and chloride reversal potential E_{Cl} values are −116 and 27 mV, respectively. Records obtained under these conditions at an applied potential of 100 mV revealed transient outward currents consistent with ion channel activity (Fig. 5*A*). At an astrocytic membrane potential of −80 mV (Ruminot et al., 2011), this applied potential translates into a nominal patch potential of 20 mV, which is well above $E_{lactate}$ but below E_{Cl}. The only ion species capable of carrying this current is lactate, as chloride and sodium movements would generate inward currents. Accordingly, the currents became progressively smaller at more negative potentials (Figs. 5*A*, 6). Small inward currents were detected at a nominal patch potential of −80 mV (Fig. 6), suggesting that the channel also allows chloride to pass. For simplicity, we will use the term "lactate channel" to refer to this lactate-permeable channel. At a 40 mV nominal patch potential, the single-channel conductance of the lactate channel was 37 ± 6 pS ($n = 6$). Currents were detected in ~50% of the patches examined. It was not possible to test the effect of cell depolarization with high $[K^+]_o$, as this maneuver destabilized the patch and prevented reliable current determinations. However, cell depolarization by adding Ba^{2+} to the superfusate stabilized the patch, permitting prolonged experiments to be performed. Within seconds of exposure to Ba^{2+}, the open probability of the channel became significantly higher regardless of basal activity (Fig. 5*B*). Surprisingly, the activity of the channel was further increased when cells were superfused with a solution containing a higher concentration of lactate (Fig. 5*C*). The stimulatory effects of Ba^{2+} and lactate on channel activity were additive and reverted upon removal from the bathing solution, but

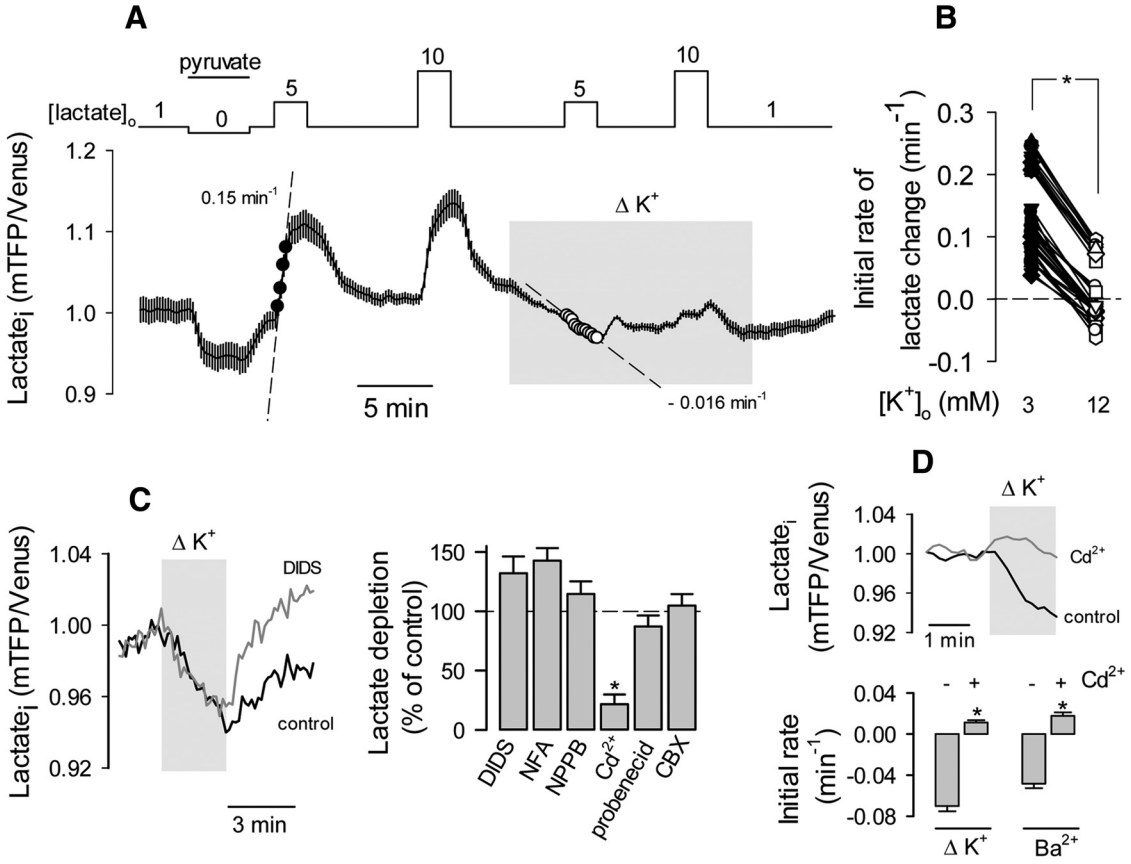

Figure 7. Stimulated astrocytes can extrude lactate against a lactate gradient. ***A***, Astrocytes were sequentially exposed to 10 mM pyruvate and then to 5 and 10 mM lactate in the presence of 3 or 12 mM $[K^+]_o$. ***B***, Summary of three similar experiments showing the initial rates of 5 mM lactate accumulation in 3 or 12 mM $[K^+]_o$. ***C***, Left, The effect of a 9 mM increase in $[K^+]_o$ on intracellular lactate was monitored in a single astrocyte before and during exposure to 200 μM DIDS. Right, Summary of similar experiments, with 200 μM DIDS, 500 μM NFA, 500 μM NPPB, 200 μM Cd^{2+}, 1 mM probenecid, or 10 μM CBX. Data are the rates of lactate depletion measured over 2 min ($n = 3$ experiments and 16–32 cells were used for each inhibitor). ***D***, Top, The effects of a 9 mM increase in $[K^+]_o$ or the addition of 3 mM Ba^{2+} on intracellular lactate level were monitored in single astrocytes before and during exposure to 200 μM Cd^{2+}. Bottom, Initial rates measured during the first minute of exposure to $[K^+]_o$ or 3 mM Ba^{2+} in the absence or presence of 200 μM Cd^{2+}.

this reversion was partial, at least over a period of minutes (Figs. 5*D*, 6).

MCTs are responsible for the lactate permeability of resting astrocytes (Barros and Deitmer, 2010; Bouzier-Sore and Pellerin, 2013; Stobart and Anderson, 2013). The high permeability of astrocytes to lactate is illustrated in Figure 7*A* as a rapid accumulation of cytosolic lactate in response to high extracellular lactate. However, when high lactate was applied in the presence of high $[K^+]_o$, the rise in lactate was smaller than that seen under resting conditions (Fig. 7*A*,*B*). In ~50% of cells, the 5 mM lactate pulse provoked intracellular lactate depletion (Fig. 7*A*,*B*). The latter result is highly informative as it means that despite high levels of extracellular lactate, efflux through the channel may still surpass influx through MCTs. It also means that the positive modulation of the channel by lactate, as described electrophysiologically, must occur at an extracellular site. The cell-attached configuration is not amenable to pharmacological characterization, so we used the initial depletion detected with the FRET nanosensor as a readout of channel activity. Considering the negative charge of lactate and the possible chloride current detected at 0 mV applied potential (Fig. 6), we tested a panel of anion channel blockers but found that only Cd^{2+} was able to inhibit K^+-induced lactate depletion to a significant extent (Fig. 7*C*). The pannexin channel blocker probenecid and the connexin hemichannel blocker CBX were not effective (Fig. 7*C*). On closer inspection, it became apparent that Cd^{2+} strongly inhibited lactate depletion immediately after the application of K^+ or Ba^{2+}, but that its effect became weaker over time (Fig. 7*D*). This suggests that there may be more than one pathway involved, and that the Cd^{2+}-sensitive channel is responsible for the early phase of the lactate release.

Discussion

The main finding of this study is that astrocytes release lactate via an ion channel in response to a small rise in extracellular K^+. The lactate-permeable channel was positively modulated by lactate itself. Resting astrocytes were found to accumulate lactate well above MCT thermodynamic equilibrium: a dynamic reservoir that was quickly mobilized in response to high $[K^+]_o$. Astrocytes are therefore equipped with a mechanism for the targeted delivery of lactate, which fits well to the emerging role of lactate as a signaling molecule (Fig. 8).

The transport of lactate across the plasma membrane of astrocytes and most other mammalian cells is mediated by H^+-coupled monocarboxylate transporters (Halestrap and Price, 1999; Barros and Deitmer, 2010; Bouzier-Sore and Pellerin, 2013; San Martín et al., 2013; Stobart and Anderson, 2013). Standard uptake assays based on isotopic tracers or pH-sensitive dyes show that lactate permeability of astrocytes is high, and no significant lactate gradients have been presumed to exist across the plasma membrane. With the FRET nanosensor, we were able to estimate lactate in the steady state and found that most astrocytes maintained lactate levels above thermodynamic equilibrium. In re-

sponse to high $[K^+]_o$ cytosolic lactate levels fell despite strong concurrent stimulation of glucose consumption. Pyruvate levels were almost unaffected, suggesting a close match between increased pyruvate production from glucose and pyruvate consumption by LDH, driven by a lower lactate level and an increased NADH/NAD^+ ratio. The K^+-dependent lactate depletion appears to be a robust phenomenon, as it was observed in both primary cultures and in protoplasmic astrocytes of adult brain slices. It has also been recorded in organotypical hippocampal slices (I. Ruminot and J.W. Deitmer, unpublished data). Also, within seconds of K^+ stimulation, a sniffer cell detected the release of lactate by astrocytes. Both lactate depletion and release were mimicked by Ba^{2+}, a maneuver that does not engage K^+ transporters (Gatto et al., 2007), suggesting that the phenomenon is chiefly mediated by membrane depolarization. In living animals, electrical stimulation of the somatosensory cortex triggered a complex astrocytic lactate response, with an initial dip and a delayed overshoot. As lactate modulates astrocytic glycolysis within seconds (Sotelo-Hitschfeld et al., 2012), the lactate dip may contribute to the stimulation of glycolysis by high $[K^+]_o$. Although the depletion phase of the lactate dip observed in protoplasmic astrocytes *in vivo* correlates with the K^+-dependent depletion observed in cultured astrocytes and in protoplasmic astrocytes *in vitro*, and we could mimic both dip and overshoot under culture conditions, the extent to which the lactate dip *in vivo* is mediated by K^+ is not clear at this stage. Electrical stimulation increases interstitial K^+ and depolarizes astrocytes (Fröhlich et al., 2008), but also mobilizes other mediators that may affect lactate metabolism. The combination of cytosolic depletion and release is evidence of increased lactate permeability, an outcome that could not be ascribed to the MCTs, as pharmacological MCT blockage failed to prevent lactate depletion. Both the depletion of cytosolic lactate by high $[K^+]_o$ and the further depletion during a lactate pulse could be explained by the electrophysiological detection of a lactate-permeable ion channel, having an open probability increased by plasma membrane depolarization and by lactate. The lactate channel was not detected in the whole-cell configuration, suggesting the need for an intact intracellular milieu. Considering that the application of high lactate concentrations to K^+-stimulated cells caused a decrease in intracellular lactate levels, the modulation of the channel by lactate seems to occur at the cell surface. One possible explanation may be direct gating of the channel by the permeant ion, a phenomenon that has already been described for anion channels (Pusch and Jentsch, 1994; Catalán et al., 2004).

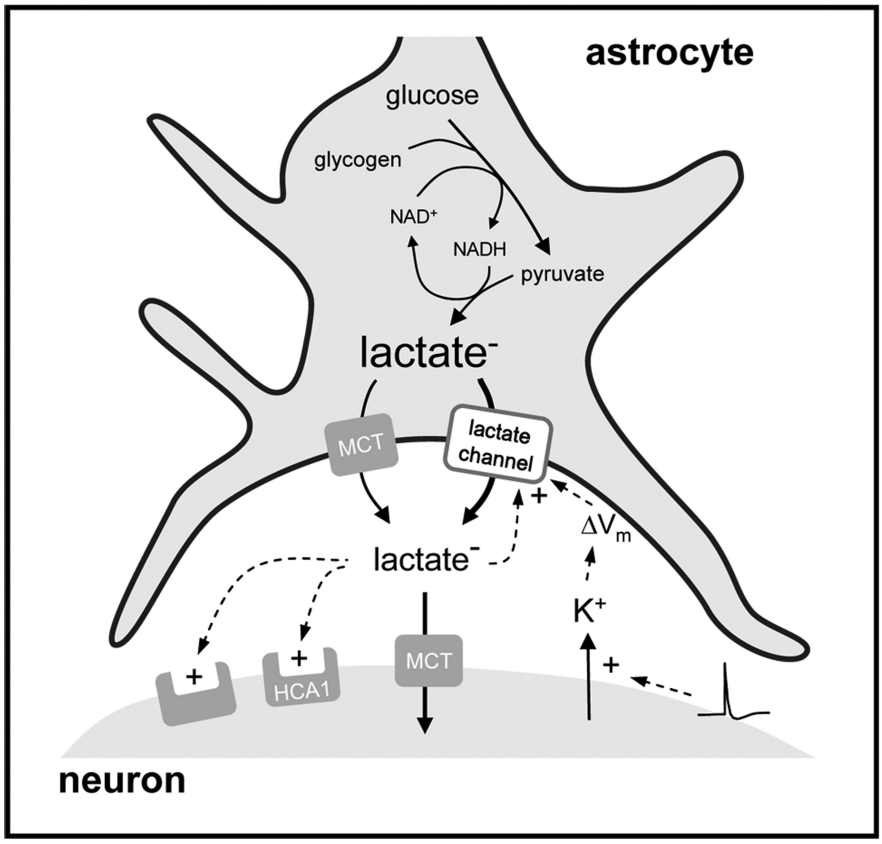

Figure 8. Activity-dependent channel-mediated lactate release by astrocytes. Resting astrocytes maintain a standing reservoir of cytosolic lactate, the result of a dynamic balance between glycolytic production and MCT-mediated lactate export. Active neurons release K^+, which depolarizes the astrocytic plasma membrane (ΔV_m) and activates the lactate-permeable channel, resulting in lactate release, leading to higher $[lactate]_o$ and further lactate release through a positive feedback. Neurons may sense lactate through HCA1 (Bozzo et al., 2013; Lauritzen et al., 2013) and other surface lactate receptors (Tang et al., 2014), or after internalization of lactate via MCTs.

To the best of our knowledge, there are no previous reports of lactate-permeable ion channels in astrocytes. The lactate-permeable channel of astrocytes was insensitive to 4,4′-diisothiocyano-2,2′-stilbenedisulfonic acid (DIDS), niflumic acid (NFA), 5-nitro-2-(3-phenylpropylamino)benzoic acid (NPPB), probenecid, and carbenoxolone (CBX), but was partially inhibited by Cd^{2+}, a nonspecific ion channel inhibitor. Anion channels are notoriously insensitive to inhibitors (Kimelberg et al., 2006), which has made it very difficult to link functionally identified anion channels to their molecular counterparts (Jentsch et al., 2002). However, a breakthrough was made recently with the molecular identification of the volume-regulated anion channel VRAC (Qiu et al., 2014; Voss et al., 2014). Anion channels in astrocytes are stimulated by ATP, cell swelling, shape changes, and other stimuli (Kimelberg et al., 2006), but we found no information on astrocytic anion channels activated by cell depolarization. This may be because electrophysiological measurements are normally performed in whole-cell voltage clamp, a configuration in which the lactate channel did not appear. It was, however, readily found in the cell-attached patch-clamp configuration, suggesting the need for a cytosolic factor that may be lost during dialysis. The main substrate of anion channels is chloride, but some of these channels may also transport large zwitterionic polyions such as taurine (125 Da; Qiu et al., 2014; Voss et al., 2014), and are therefore likely to transport lactate, a smaller monovalent anion (88 Da). Lactate has not been routinely included in selectivity studies of anion channels. The maxi-anion channel is present in astrocytes (Kimelberg et al., 2006), but its conductance seems too large (>300 pS for chloride, and presumably >100 pS for lactate) to account for the lactate permeability described here. Conductance may also be invoked

against connexins and pannexins (>200 pS; Giaume et al., 2013), together with the observed insensitivity of the lactate channel to carbenoxolone and probenecid, and the fact that connexins and pannexins are permeable to cations.

An activity-dependent lactate channel in astrocytes has consequences for brain lactate dynamics. There are fundamental differences between the standard transport of lactate via MCTs and transport via an ion channel; one of these is vectorial flux. Lactate is a monovalent anion, and at the resting membrane potential of astrocytes (−80 mV) lactate will flow through the channel against a 20-fold chemical gradient. At 12 mM $[K^+]_o$, the membrane potential of a "depolarized" astrocyte is still −60 mV (Ruminot et al., 2011), a voltage at which channel-mediated efflux will occur against a 10-fold chemical gradient. This explains how an imposed fivefold rise in extracellular lactate failed to increase intracellular lactate levels in K^+-stimulated astrocytes (Fig. 3*E*). In contrast, MCT-mediated transport is electroneutral and may only extrude lactate if there is a favorable combined chemical gradient for lactate and H^+. During neural activity, astrocytes become more alkaline and neurons acidify (Chesler, 2003), a combination that works against the transfer of lactate from astrocytes to neurons (Barros and Deitmer, 2010). Using a pathway that is H^+ independent and sensitive to membrane potential, astrocytes may push lactate toward neurons regardless of the pH gradient, even if lactate has accumulated in the interstice. Another relevant property of channels is their unmatched throughput rate. Assuming linear dose dependence, we can calculate that a single 37 pS channel (adjusted at 1.4 mM and −60 mV) conducts $>10^5$ lactate molecules per second, about a thousand times faster than the maximum turnover number of MCT1 (Ovens et al., 2010). Astrocytic lactate has been proposed to serve as an energy substrate for active neurons, a mechanism known as the astrocyte-to-neuron lactate shuttle (ANLS; Pellerin and Magistretti, 1994; Bouzier-Sore and Pellerin, 2013; Stobart and Anderson, 2013). In its standard version, ANLS is mediated by MCTs, and therefore the direction of flux is determined by the lactate gradient between both cells, which is unknown (Barros and Deitmer, 2010). The lactate channel strengthens the ANLS by providing obligatory vectorial flux (energized by the astrocytic membrane potential), activity dependence (mediated by $[K^+]_o$), and a much higher throughput rate.

In addition to a role in neurometabolic coupling, the lactate channel may contribute to intercellular signaling. The G_i-protein-coupled receptor for lactate HCA1 (GPR81) was recently described in synaptic regions, perivascular locations, and glia (Bergersen and Gjedde, 2012; Lauritzen et al., 2013), whereas the engagement of HCA1 in cortical neurons in culture reduced their spontaneous activity (Bozzo et al., 2013). In the locus ceruleus, astrocytic lactate was found to excite neurons, a phenomenon mediated by a different surface lactate receptor (Tang et al., 2014). After entering neurons, lactate affects pH, the NADH/NAD^+ ratio, and the energy status, modulating enzyme catalysis, gene expression, and higher-order brain functions like memory consolidation (Gilbert et al., 2006; Suzuki et al., 2011; Barros, 2013; Yang et al., 2014). Because of the delicate geometry of protoplasmic astrocytes, their membrane potential is thought to be a local parameter, exquisitely sensitive to fluctuations in $[K^+]_o$ (Kofuji and Newman, 2004; Fröhlich et al., 2008; Witthoft et al., 2013). Depending on location, the lactate channel may sense the local rise in $[K^+]_o$ that accompanies excitatory neurotransmission and perhaps the activity of the nodes of Ranvier, which are contacted by astrocytic processes. A single channel may deliver lactate transiently as a localized jet, permitting accurate homing of targets in neighboring cells and/or in autocrine fashion. The amplification conferred by the positive feedback modulation of the channel by lactate is expected to make the release even more abrupt. Astrocytes detect synaptic activity through metabotropic and ionotropic glutamate receptors, leading to the release of glutamate, ATP, and D-serine, small neuromodulators that are collectively termed gliotransmitters (Araque et al., 2014). Astrocytes can also detect synaptic activity through changes in local $[K^+]_o$. The neuromodulatory roles of lactate, its steady-state reservoir in astrocytes, and its fast release in response to K^+, suggest that lactate may also qualify as a gliotransmitter.

References

Araque A, Carmignoto G, Haydon PG, Oliet SH, Robitaille R, Volterra A (2014) Gliotransmitters travel in time and space. Neuron 81:728–739. CrossRef Medline

Barros LF (2013) Metabolic signaling by lactate in the brain. Trends Neurosci 36:396–404. CrossRef Medline

Barros LF, Deitmer JW (2010) Glucose and lactate supply to the synapse. Brain Res Rev 63:149–159. CrossRef Medline

Barros LF, Baeza-Lehnert F, Valdebenito R, Ceballo S, Alegría K (2014) Fluorescent nanosensor based flux analysis: overview and the example of glucose. In: Springer protocols: brain energy metabolism (Waagepetersen HS, Hirrlinger J, eds), pp 145–159. Berlin: Springer.

Barry PH (1994) JPCalc, a software package for calculating liquid junction potential corrections in patch-clamp, intracellular, epithelial and bilayer measurements and for correcting junction potential measurements. J Neurosci Methods 51:107–116. CrossRef Medline

Bekar LK, Walz W (2002) Intracellular chloride modulates A-type potassium currents in astrocytes. Glia 39:207–216. CrossRef Medline

Bergersen LH, Gjedde A (2012) Is lactate a volume transmitter of metabolic states of the brain? Front Neuroenergetics 4:5. CrossRef Medline

Bittner CX, Loaiza A, Ruminot I, Larenas V, Sotelo-Hitschfeld T, Gutiérrez R, Córdova A, Valdebenito R, Frommer WB, Barros LF (2010) High resolution measurement of the glycolytic rate. Front Neuroenergetics 2:26. CrossRef Medline

Bittner CX, Valdebenito R, Ruminot I, Loaiza A, Larenas V, Sotelo-Hitschfeld T, Moldenhauer H, San Martín A, Gutiérrez R, Zambrano M, Barros LF (2011) Fast and reversible stimulation of astrocytic glycolysis by K^+ and a delayed and persistent effect of glutamate. J Neurosci 31:4709–4713. CrossRef Medline

Bouzier-Sore AK, Pellerin L (2013) Unraveling the complex metabolic nature of astrocytes. Front Cell Neurosci 7:179. CrossRef Medline

Bozzo L, Puyal J, Chatton JY (2013) Lactate modulates the activity of primary cortical neurons through a receptor-mediated pathway. PLoS One 8:e71721. CrossRef Medline

Catalán M, Niemeyer MI, Cid LP, Sepúlveda FV (2004) Basolateral ClC-2 chloride channels in surface colon epithelium: regulation by a direct effect of intracellular chloride. Gastroenterology 126:1104–1114. CrossRef Medline

Chesler M (2003) Regulation and modulation of pH in the brain. Physiol Rev 83:1183–1221. CrossRef Medline

Choi HB, Gordon GR, Zhou N, Tai C, Rungta RL, Martinez J, Milner TA, Ryu JK, McLarnon JG, Tresguerres M, Levin LR, Buck J, MacVicar BA (2012) Metabolic communication between astrocytes and neurons via bicarbonate-responsive soluble adenylyl cyclase. Neuron 75:1094–1104. CrossRef Medline

Davidson S, Truong H, Nakagawa Y, Giesler GJ Jr (2010) A microinjection technique for targeting regions of embryonic and neonatal mouse brain in vivo. Brain Res 1307:43–52. CrossRef Medline

Dirren E, Towne CL, Setola V, Redmond DE Jr, Schneider BL, Aebischer P (2014) Intracerebroventricular injection of adeno-associated virus 6 and 9 vectors for cell type-specific transgene expression in the spinal cord. Hum Gene Ther 25:109–120. CrossRef Medline

Fröhlich F, Bazhenov M, Iragui-Madoz V, Sejnowski TJ (2008) Potassium dynamics in the epileptic cortex: new insights on an old topic. Neuroscientist 14:422–433. CrossRef Medline

Gatto C, Arnett KL, Milanick MA (2007) Divalent cation interactions with Na, K-ATPase cytoplasmic cation sites: implications for the para-nitrophenyl phosphatase reaction mechanism. J Membr Biol 216:49–59. CrossRef Medline

Giaume C, Leybaert L, Naus CC, Sáez JC (2013) Connexin and pannexin

hemichannels in brain glial cells: properties, pharmacology, and roles. Front Pharmacol 4:88. CrossRef Medline

Gilbert E, Tang JM, Ludvig N, Bergold PJ (2006) Elevated lactate suppresses neuronal firing in vivo and inhibits glucose metabolism in hippocampal slice cultures. Brain Res 1117:213–223. CrossRef Medline

Halestrap AP, Price NT (1999) The proton-linked monocarboxylate transporter (MCT) family: structure, function and regulation. Biochem J 343: 281–299. Medline

Hof PR, Pascale E, Magistretti PJ (1988) K^+ at concentrations reached in the extracellular space during neuronal activity promotes a Ca^{2+}-dependent glycogen hydrolysis in mouse cerebral cortex. J Neurosci 8:1922–1928. Medline

Hou BH, Takanaga H, Grossmann G, Chen LQ, Qu XQ, Jones AM, Lalonde S, Schweissgut O, Wiechert W, Frommer WB (2011) Optical sensors for monitoring dynamic changes of intracellular metabolite levels in mammalian cells. Nat Protoc 6:1818–1833. CrossRef Medline

Hu Y, Wilson GS (1997) A temporary local energy pool coupled to neuronal activity: fluctuations of extracellular lactate levels in rat brain monitored with rapid-response enzyme-based sensor. J Neurochem 69:1484–1490. CrossRef Medline

Hung YP, Albeck JG, Tantama M, Yellen G (2011) Imaging cytosolic NADH-NAD(+) redox state with a genetically encoded fluorescent biosensor. Cell Metab 14:545–554. CrossRef Medline

Jakoby P, Schmidt E, Ruminot I, Gutiérrez R, Barros LF, Deitmer JW (2014) Higher transport and metabolism of glucose in astrocytes compared with neurons: a multiphoton study of hippocampal and cerebellar tissue slices. Cereb Cortex 24:222–231. CrossRef Medline

Jentsch TJ, Stein V, Weinreich F, Zdebik AA (2002) Molecular structure and physiological function of chloride channels. Physiol Rev 82:503–568. CrossRef Medline

Kimelberg HK, Macvicar BA, Sontheimer H (2006) Anion channels in astrocytes: biophysics, pharmacology, and function. Glia 54:747–757. CrossRef Medline

Kofuji P, Newman EA (2004) Potassium buffering in the central nervous system. Neuroscience 129:1045–1056. CrossRef Medline

Lauritzen KH, Morland C, Puchades M, Holm-Hansen S, Hagelin EM, Lauritzen F, Attramadal H, Storm-Mathisen J, Gjedde A, Bergersen LH (2014) Lactate receptor sites link neurotransmission, neurovascular coupling, and brain energy metabolism. Cereb Cortex 10:2784–2795. CrossRef Medline

Loaiza A, Porras OH, Barros LF (2003) Glutamate triggers rapid glucose transport stimulation in astrocytes as evidenced by real-time confocal microscopy. J Neurosci 23:7337–7342. Medline

Ovens MJ, Davies AJ, Wilson MC, Murray CM, Halestrap AP (2010) AR-C155858 is a potent inhibitor of monocarboxylate transporters MCT1 and MCT2 that binds to an intracellular site involving transmembrane helices 7–10. Biochem J 425:523–530. CrossRef Medline

Pellerin L, Magistretti PJ (1994) Glutamate uptake into astrocytes stimulates aerobic glycolysis: a mechanism coupling neuronal activity to glucose utilization. Proc Natl Acad Sci U S A 91:10625–10629. CrossRef Medline

Pologruto TA, Sabatini BL, Svoboda K (2003) ScanImage: flexible software for operating laser scanning microscopes. Biomed Eng Online 2:13. CrossRef Medline

Prichard J, Rothman D, Novotny E, Petroff O, Kuwabara T, Avison M, Howseman A, Hanstock C, Shulman R (1991) Lactate rise detected by 1H NMR in human visual cortex during physiologic stimulation. Proc Natl Acad Sci U S A 88:5829–5831. CrossRef Medline

Pusch M, Jentsch TJ (1994) Molecular physiology of voltage-gated chloride channels. Physiol Rev 74:813–827. Medline

Qiu Z, Dubin AE, Mathur J, Tu B, Reddy K, Miraglia LJ, Reinhardt J, Orth AP, Patapoutian A (2014) SWELL1, a plasma membrane protein, is an essential component of volume-regulated anion channel. Cell 157:447–458. CrossRef Medline

Ruminot I, Gutiérrez R, Peña-Münzenmayer G, Añazco C, Sotelo-Hitschfeld T, Lerchundi R, Niemeyer MI, Shull GE, Barros LF (2011) NBCe1 mediates the acute stimulation of astrocytic glycolysis by extracellular K^+. J Neurosci 31:14264–14271. CrossRef Medline

San Martín A, Ceballo S, Ruminot I, Lerchundi R, Frommer WB, Barros LF (2013) A genetically encoded FRET lactate sensor and its use to detect the warburg effect in single cancer cells. PLoS One 8:e57712. CrossRef Medline

San Martín A, Ceballo S, Baeza-Lehnert F, Lerchundi R, Valdebenito R, Contreras-Baeza Y, Alegría K, Barros LF (2014a) Imaging mitochondrial flux in single cells with a FRET sensor for pyruvate. PLoS One 9:e85780. CrossRef Medline

San Martín A, Sotelo-Hitschfeld T, Lerchundi R, Fenandez-moncada I, Ceballo S, Valdebenito R, Baeza-Lehnert F, Alegria K, Contreras-Baeza Y, Garrido-Gerter P, Romero-Gomez I, Barros LF (2014b) Single-cell imaging tools for brain energy metabolism: a review. Neurophotonics 1:011004. CrossRef

Sotelo-Hitschfeld T, Fernández-Moncada I, Barros LF (2012) Acute feedback control of astrocytic glycolysis by lactate. Glia 60:674–680. CrossRef Medline

Stobart JL, Anderson CM (2013) Multifunctional role of astrocytes as gatekeepers of neuronal energy supply. Front Cell Neurosci 7:38. CrossRef Medline

Suzuki A, Stern SA, Bozdagi O, Huntley GW, Walker RH, Magistretti PJ, Alberini CM (2011) Astrocyte-neuron lactate transport is required for long-term memory formation. Cell 144:810–823. CrossRef Medline

Takanaga H, Chaudhuri B, Frommer WB (2008) GLUT1 and GLUT9 as major contributors to glucose influx in HepG2 cells identified by a high sensitivity intramolecular FRET glucose sensor. Biochim Biophys Acta 1778:1091–1099. CrossRef Medline

Tang F, Lane S, Korsak A, Paton JF, Gourine AV, Kasparov S, Teschemacher AG (2014) Lactate-mediated glia-neuronal signalling in the mammalian brain. Nat Commun 5:3284. CrossRef Medline

Tantama M, Hung YP, Yellen G (2012) Optogenetic reporters: fluorescent protein-based genetically encoded of signaling and metabolism in the brain. In: Progress in brain research (Knopfel T, Boyden E, eds), pp 235–263. Amsterdam: Elsevier.

Voss FK, Ullrich F, Münch J, Lazarow K, Lutter D, Mah N, Andrade-Navarro MA, von Kries JP, Stauber T, Jentsch TJ (2014) Identification of LRRC8 heteromers as an essential component of the volume-regulated anion channel VRAC. Science 344:634–638. CrossRef Medline

Witthoft A, Filosa JA, Karniadakis GE (2013) Potassium buffering in the neurovascular unit: models and sensitivity analysis. Biophys J 105:2046–2054. CrossRef Medline

Yang J, Ruchti E, Petit JM, Jourdain P, Grenningloh G, Allaman I, Magistretti PJ (2014) Lactate promotes plasticity gene expression by potentiating NMDA signaling in neurons. Proc Natl Acad Sci U S A 111:12228–12233. CrossRef Medline